

Online Covariate Shift Detection based Adaptive Brain-Computer Interface to Trigger Hand Exoskeleton Feedback for Neuro-Rehabilitation

Anirban Chowdhury, *Student Member, IEEE*, Haider Raza, *Member, IEEE*, Yogesh Kumar Meena, *Student Member, IEEE*, Ashish Dutta, *Member, IEEE*, and Girijesh Prasad, *Senior Member, IEEE*

Abstract—A major issue in electroencephalogram (EEG) based brain-computer interfaces (BCIs) is the intrinsic non-stationarities in the brain waves, which may degrade the performance of the classifier, while transitioning from calibration to feedback generation phase. The non-stationary nature of the EEG data may cause its input probability distribution to vary over time, which often appear as a covariate shift. To adapt to the covariate shift, we had proposed an adaptive learning method in our previous work and tested it on offline standard datasets. This paper presents an online BCI system using previously developed covariate shift detection (CSD)-based adaptive classifier to discriminate between mental tasks and generate neurofeedback in the form of visual and exoskeleton motion. The CSD test helps prevent unnecessary retraining of the classifier. The feasibility of the developed online-BCI system was first tested on 10 healthy individuals, and then on 10 stroke patients having hand disability. A comparison of the proposed online CSD-based adaptive classifier with conventional non-adaptive classifier has shown a significantly ($p \leq 0.01$) higher classification accuracy in both the cases of healthy and patient groups. The results demonstrate that the online CSD-based adaptive BCI system is superior to the non-adaptive BCI system and it is feasible to be used for actuating hand exoskeleton for the stroke-rehabilitation applications.

Index Terms—Adaptive learning, Brain-computer interface, Covariate shift detection, Hand-exoskeleton, Neurorehabilitation.

I. INTRODUCTION

SINCE its inception in 1973 by J.J. Vidal, brain-computer interface (BCI) technology has seen a rapid growth in the last three decades, thanks to the advancement in neurophysiology, electronics, signal processing, and computer science [1]. The BCI technology has found its utility as a potential means of communication and control for disabled people to interact with the outside world [2]. Several features extracted from the cortical signals such as the slow cortical potentials, sensory motor rhythms (SMR), and P300, have been exploited to make several applications using the BCI systems [3].

As BCI requires focused attention which is also a key factor in regenerating motor skills, many neurorehabilitation therapies have been designed using this technology [4], [5].

AC and AD are with the Centre of Mechatronics, Indian Institute of Technology (IIT) Kanpur, India

HR is with School of Computer Science and Electronic Engineering, University of Essex, UK

YKM and GP are with Intelligent Systems Research Centre, Ulster University, UK

Corresponding authors: AC (anir@iitk.ac.in)

Manuscript received June XX, 2017; revised Month XX, 201X.

These therapies have a potential for faster regeneration and reorganization of the neuronal networks, often known as neuroplasticity [6]. The strong correlation between EEG signals and mental tasks has led to many user centric applications such as virtual spellers for the communication [7], functional electrical stimulation (FES) based neuro-prosthesis for tetraplegics [4], hand exoskeleton control [8], [9], [10], [11] and telepresence for personal assistance [12]. In spite of the seemingly bright prospect of the BCI technology, there are some practical challenges regarding the robustness, accuracy, and information transfer rate (ITR) of such systems [13], [14], [15]. The non-stationary nature of neurophysiological signals and dynamics of brain activity make the EEG-based BCI, a dynamically varying system, and thus improving its learning performance is a challenging task [16]. It is well-known that due to the presence of non-stationarity, the input data distribution of EEG varies from trial-to-trial and also from session-to-session transfer. The non-stationarities of the EEG signals may be caused by various reasons such as changes in the user attention level, electrode placement, and user fatigue [17]. As a result, these variations often appear as covariate shifts, wherein the input data distributions differ significantly between training/calibration and evaluation/online feedback phases, while the conditional distribution remains the same [18]. Within an EEG-based BCI system that operates online in real-time non-stationary/changing environments, learning approaches are needed that can track the changes over time, and adapt in a timely fashion. The BCI systems, wherein the users are trained to produce a fixed EEG pattern, are often time-consuming and tiring for the participants [13], while the advent of Berlin BCI system greatly shortened the subject specific training protocols by the use of machine learning techniques [19], [20], [21]. Thus, it speeds up the conventional training protocols for improved performance [13], and could be more natural and relevant for people with disability [4]. Adaptive Brain Interface (ABI) was one of the earliest examples of such BCI systems [17], later many other systems using error potential based adaptation [22], adaptive autoregressive models [23], transductive learning [24], covariate shift adaptation [18], [25], Kullback-Leiber-Common-Spatial-Patterns (KLCSP) [26], interval-type-2-fuzzy classifiers [27] have been implemented.

However, there is always a risk for inappropriate adaptation, wherein the user may be confused by the unpredictable changes which may lead to degraded performance

[22]. Although the common spatial patterns (CSP) based feature extraction method has been widely explored to compute spatial filters which give maximum feature separability, they are not invariant against dynamic intra- and inter-session changes in the signal, as CSP only considers the difference in means between two classes while ignoring the scatter within a particular class [20], [28]. Next, Li et al., [18] proposed a covariate shift adaptation (CSA) method for improving the performance of BCI systems. Additionally, a covariate shift minimization (CSM) method was proposed for the non-stationary adaptation to reduce the feature set overlap and unbalance for different classes in the feature set domain [29]. Also, most of the covariate shift adaptation (CSA) methods are commonly implemented in a batch processing manner, which limits its applicability in real-time application [29], [18], [30]. It is important to note that the non-stationary adaptation methods are majorly categorized into passive and active approaches [31]. However, the traditional BCI systems are based on passive approach for non-stationary learning in EEG. In contrast, an active approach based non-stationary learning method in BCI system may be a possible option that uses a CSD test to detect the presence of covariate shifts in the streaming EEG features, and based upon the detected shift, an adaptive action is initiated. In our previous work [16], we have implemented the active approach in single-trial EEG classification in offline mode and the performance of the system was superior to existing passive approach based BCI systems [32], [17], [29], [18], [33], [34]. However, improving the accuracy of the online BCI system for the neurorehabilitation purpose is still an open challenge.

Here we present an online adaptive BCI system based on a two-stage CSD test. In the first stage of online CSD test, it generates a shift detection warning using the exponentially weighted moving average (EWMA) model and in the second stage, this warning is validated by Hotelling's T-square statistical test. The second stage of the CSD test aims to reduce the false detection rates [35], [36]. A combination of CSD test and supervised adaptation helps to build an online adaptive BCI system that aims to trigger a hand exoskeleton device to provide a neurofeedback for healthy volunteers, and stroke patients suffering from finger impairment. We have chosen this specific area of disability as EEG pattern recognition for finger movements is relatively challenging due to low signal-to-noise ratio (SNR) and finger representative areas in the somatosensory cortex are spatially over-lapping [37]. Also, there is a need for undertaking such work because BCI systems requiring quick calibration and user adaptation in real-time are in high demand, while there is a real shortage of such studies on stroke patients [38]. The key contributions of the research in the paper are summarized as follows:

- 1) *It implements an online adaptive BCI system and tests it for feasibility on healthy and post-stroke individuals.*
- 2) *For user-specific adaptation, the system uses the two stage CSD-based adaptation technique, which reduces the rate of false shift and is applicable to online streaming data.*
- 3) *It uses two feedback modes: visual feedback is given*

on computer screen and proprioceptive feedback is provided through a hand exoskeleton, which also motivates the user, for adapting to the system. Thus it facilitates mutual learning.

- 4) *The performance of the proposed system is demonstrated to be superior to the conventional system non-adaptive classifier.*

The remainder of this paper proceeds as follows: Section II presents materials and methods that include system overview, experimental protocol, data acquisition, and signal processing for the proposed adaptive BCI system. Next, section III presents the performance analysis and results. Finally, Section IV includes the discussion and section V summarizes the findings of this study.

II. MATERIALS AND METHODS

A. System Overview

The adaptive BCI system developed for the experimentation, uses g.USBamp (g.tec, Graz, Austria) biosignal amplifier, EEG cap (g.tec), Ag/AgCl based EEG electrodes for recording scalp EEG data. The experimental paradigm and software for the signal processing and feedback generation were built in-house using MATLAB-Simulink environment. The neurofeedback was provided in the form of a visual hand grasp on the computer screen and actual motion of the same grasping action was provided using a hand-exoskeleton for moving coupled index-middle fingers and thumb.

The exoskeleton was developed using a nylon based light weight material by a rapid prototyping method and it is portable and comfortable to wear [39]. It does the flexion and extension motion of the fingers for the patients suffering from finger impairment after stroke. The index and middle fingers are coupled and a four-bar mechanism drives them jointly. Although they are coupled, the finger attachments are made in such a manner, that it doesn't put unnecessary pressure on the fingers. For driving the thumb, there is another four-bar mechanism. The four-bar linkages are driven by servo motors in position control mode for following a predefined human finger trajectory of flexion and extension motion.

B. Experimental Protocol

An overview of the experimental protocol is shown in Fig. 1. It follows a conventional SMR BCI architecture consisting of two stages. The first stage is the data acquisition without giving any feedback, from which an initial classifier is trained using the extracted features and the initial parameters for CSD based classifier adaptation is obtained. This is followed by the online BCI stage that issues neurofeedback on the basis of the classifier outputs. Data acquisition during first stage consists of two runs of 40 trials and each run takes about 7 minutes and 30 seconds. Next, the classifier was trained in the off-line mode and it takes nearly 30 s, which is followed by one feedback run of 40 trials in online BCI mode. In each run 20 trials are left and remaining 20 trials are right hand MI. Therefore it is a balanced classification problem where the chance accuracy of the classifier is 50%. This transition from calibration to feedback stage nearly takes only 16 mins, which is desirable in a rehabilitation scenario, as patients may get tired and loose

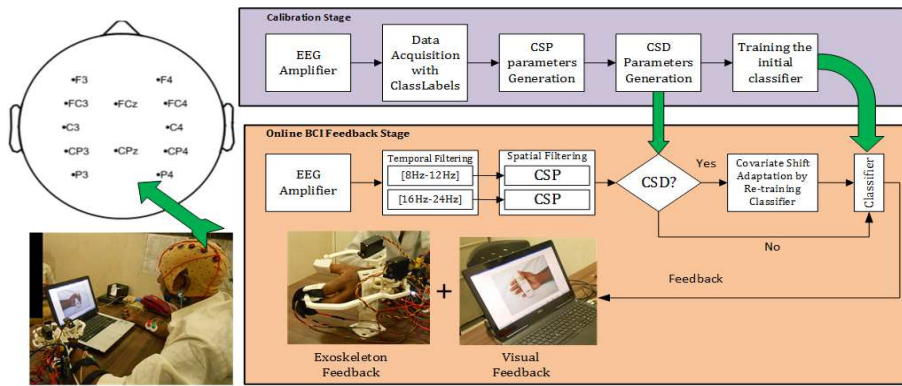


Fig. 1. An overview of the experimental protocol showing the EEG electrode placements (top-left); calibration, and online feedback generation stages (right) and also the participant interacting with the BCI system (bottom-left).

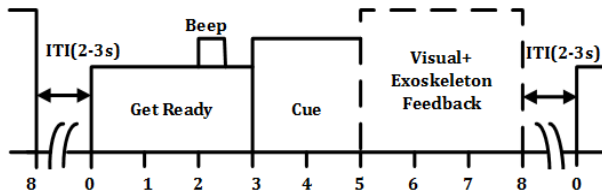


Fig. 2. Timing diagram of a trial during online BCI run. Here feedback trigger time instant (FTTI) = 5. The FTTI is not fixed but it varies depending upon the selection of suitable time segment from the calibration phase. A time-segment of 1.5 s before the FTTI is used for feature extraction, CSD test and feedback trigger generation.

attention if the session is excessively longer. Each trial period in the calibration phase was of 8 s (similar to that shown in the timing paradigm of online BCI in Fig. 2), within which first three seconds was the preparatory phase where a message stating “Get Ready” appeared in the middle of a computer screen. After a 2 s period, a beep sound occurred and then at the end of the 3rd second, a cue in the form of a hand-image appeared on the screen, either on the left or in the right side. According to the appearance of the cue, the participants were instructed to perform an MI task of a left or right-hand grasp. In the calibration stage, the cue lasted up to the end of 8th second, after which the screen goes blank for a random period of 2 s to 3 s before the start of another trial. The acquired EEG signals along with the class-labels are then fed into a feature extraction module, which extracts the CSP features to train a support vector machine (SVM) classifier with linear kernel and also calculates the CSD parameters, later to be used in the online-feedback BCI phase for adapting the classifier. The process of feature extraction and classifier training was done by taking a sliding window of 1.5 s and shifted in steps of 0.5 s to find out the interval of maximum decoding accuracy by means of a randomized 10 fold cross-validation. This interval was then locked to be used in the online evaluation stage to generate neurofeedback according to the classifier’s output. This selection of time-segment is specific to a participant. An example of the timing diagram of a trial during online BCI phase is shown in Fig. 2, where the feedback was triggered at 5 s, which means that the EEG data over the period 3.5 to 5 s was used for feature extraction in this case. The time

when the feedback was triggered is termed here as feedback trigger time instant (FTTI). Once the feedback is triggered, it takes 3 s to complete, and hence the trial ended at 8 s. FTTI varies from participant to participant, and it could take any of the following [4.5, 5.0, 5.5, . . . , 8] s time points. It is to be noted that as the feedback duration is fixed for 3 s, the trial length extends beyond 8 s if $FTTI > 5$, and the trial length is shorter than 8 s if $FTTI < 5$ s. The online BCI stage starts with the initial classifier model calculated from the calibration stage but as the trials progress, and the covariate shifts were detected, the classifier was also retrained on new features to adapt the changes in the new input data distribution.

C. Data Acquisition

Several fMRI studies have shown that the MI of the sequential hand movements involves ipsilateral cortical regions mainly in the overlapping supplementary motor area (SMA) and primary motor cortex (M1) [40]. Also a coupled fMRI and EEG study pointed out that the current sources of the finger movements are in frontal medial and parietal regions [41]. Therefore in our study the scalp EEG was recorded with 12 electrodes covering these areas at F3, FC3, C3, CP3, P3, FCz, CPz, F4, FC4, C4, CP4, and P4 locations according to 10-20 international system. Surface EMG electrodes were also placed on flexor-digitorum-superficialis (FDS) muscles in the right and left forearm to monitor any overt hand movement during MI trials. The signals were sampled at 512 Hz and initially filtered with 0.1 Hz to 100 Hz pass-band filter and a notch filter at 50 Hz during data acquisition.

D. Study Participants

10 healthy volunteers and 10 hemiplegic patients participated in the experiment. All of them had no prior experience in undergoing BCI trials. The healthy participants were in the age group of 20-50 (mean = 41 ± 9.21) years and the demographics of the participating patients are given in Table. I. The patients were recruited ensuring they had no history of epilepsy. The cognitive impairment was also checked and patients scoring at least 7/10 in Hodgekinson’s mini-mental test score were considered for the experiment [42]. The participants signed a written consent form before starting the experiments and the experimental protocol was approved by the institute ethics committee of IIT Kanpur, India.

TABLE I
DEMOGRAPHICS OF THE PATIENTS

| Participants | Age (Years) | Gender | IS (L/R) | DS (L/R) | TSS (Months) |
|--------------|-------------|--------|----------|----------|--------------|
| S01 | 48 | Male | Left | Right | 8 |
| S02 | 71 | Male | Left | Right | 20 |
| S03 | 63 | Male | Right | Right | 8 |
| S04 | 35 | Female | Right | Right | 3 |
| S05 | 24 | Male | Left | Right | 8 |
| S06 | 45 | Female | Left | Right | 6 |
| S07 | 48 | Male | Left | Right | 2 |
| S08 | 62 | Female | Left | Right | 6 |
| S09 | 28 | Male | Left | Right | 1 |
| S10 | 51 | Female | Right | Right | 48 |

IS: Impaired Side, DS: Dominant Side, TSS: Time Since Stroke
L: Left Hand, R: Right Hand

E. Methods

The EEG-based online BCI implemented using CSD-based adaptive classifier is abbreviated here as EEG-CSAC. For comparative evaluation, its decoding accuracy is compared with the case where the same classifier is not adapted (i.e. calibration stage classifier parameters remain unchanged), named as EEG-based non-adaptive classifier (EEG-NAC). The EEG-NAC only lacks the CSD-based adaptation part, while the rest are same for both the methods. It is to be noted that the online BCI was implemented only using the EEG-CSAC method and EEG-NAC was applied later in off-line mode on the same data, once the online BCI run is completed. This was done to check the decoding accuracy with and without adaptation. The methods are described as follows: First the temporal and spatial filtering, which are common to both the EEG-NAC and EEG-CSAC are described. Then the algorithm of EEG-NAC is outlined followed by the details of the additional steps relating to EEG-CSAC, which are covariate-shift detection, validation, and adaptation.

1) *Temporal and Spatial Filtering*: The recorded signals have been band-pass filtered for two frequency bands (i.e. $\mu = [8-12]$ Hz, $\beta = [16-24]$ Hz). These two frequency ranges have been chosen empirically as they provide stable frequency response for Event-Related-Desynchronization or Event-Related-Synchronization (ERD/ERS) [43]. Due to volumetric conduction raw EEG scalp potentials do not have good spatial resolution. If our signal of interest is dominated by the other sources having stronger signal in the same frequency range, EEG signal classification is affected [20]. An effective spatial filtering algorithm is common-spatial-pattern (CSP) algorithm [44]. It is an efficient tool to analyze multichannel EEG data for binary classification. It is basically a supervised decomposition of signals parameterized by a matrix $W \in R^{\{C \times C\}}$ (C: number of channels). The matrix is used to project the original sensor space E into the surrogate sensor space, using eq.(1)

$$Z = WE \quad (1)$$

where, $E \in R^{\{C \times T\}}$ is the EEG measurement of a single-trial and T is the number of samples per channel. W is the CSP

projection matrix. The rows of W are the spatial filters and the columns are the common spatial patterns. A small number of spatially filtered signals are used as features for classification purpose. These are generally first and last rows of Z , i.e. Z_t , where $t \in \{1 \dots 2m\}$. The feature vector is derived from Z_t by eq.(2) as,

$$x_t = \log \left(\frac{\text{var}(Z_t)}{\sum_{i=1}^{2m} \text{var}(Z_i)} \right) \quad (2)$$

After doing the temporal and spatial filtering, and finally taking the log variance using (2), we obtain the feature vector of 12 elements from which the first and last features are kept, ignoring the elements in between. These two elements we designate as first and second best features in Fig. 3. Thus from two different frequency bands (i.e. μ and β) we obtain four elements which forms the feature vector of 1×4 dimension for a single trial.

2) *EEG-based Non-Adaptive Classifier (EEG-NAC)*: In this, a support-vector-machine (SVM) based pattern classifier with linear kernel is built upon the common assumption that the distribution of extracted features remains stationary over time. In the EEG-NAC method initially an inductive classifier is trained on the calibration dataset that consists of labeled trials. Then, in the online BCI stage, unlabeled features from streaming data are processed sequentially for the classification. In this method, only EEG-based CSP features are considered for the classification.

3) *EEG-based Covariate Shift Adaptive Classifier (EEG-CSAC)*: The EEG-based covariate shift adaptive classifier (EEG-CSAC) belongs to the category of active learning approach [16], wherein the classifier parameters are updated at each CSD during the online feedback phase. This adaptive classifier is implemented using SVM with linear kernel. The shift-detection is performed using the covariate shift detection (CSD) test based on EWMA model [35], [36], [45]. The algorithm is provided with a calibration dataset, and a classifier f is trained. In the online BCI phase, the CSD-EWMA test is used to detect the covariate shift and the classifier f is retrained to update its classification decision boundary, and then the updated classifier f is used to classify the upcoming input data from online BCI paradigm. The interactions between the covariate shift-detection, validation, and adaptation stages are explained in Fig. 4 and in the following subsections.

a) *Covariate Shift Warning (CSW)*: The first stage in a CSD-EWMA test provides covariate shift warning in the process. It makes an initial estimate of the covariate shift (i.e. whether the actual shift has occurred) and is performed by an EWMA model. If the CSD test outcome is positive, then the second stage test gets activated, and a validation is performed in order to reduce the number of false-alarms [35]. The EWMA model is explained by the following equation,

$$z_{(i)} = \lambda x_{(i)} + (1 - \lambda) z_{(i-1)} \quad (3)$$

where, the importance of the current and historical observations is decided by the parameter $\lambda (0 < \lambda \leq 1)$. $z_{(i)}$ is the exponentially weighted moving average (EWMA) of the

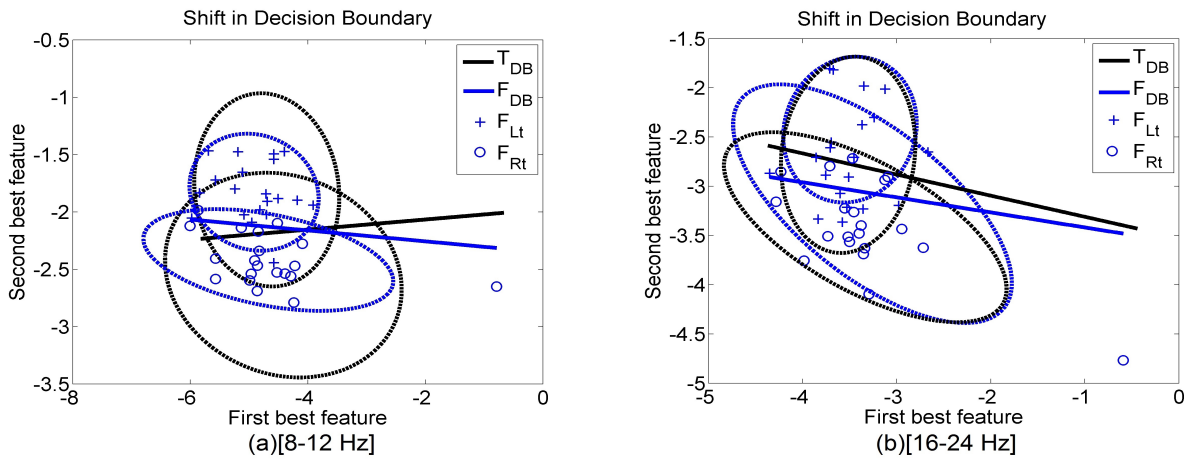


Fig. 3. Shift in the decision boundary from calibration to online feedback phase due to covariate shift, in (a) μ [8 – 12 Hz] band and (b) β [16 – 24 Hz] band for healthy participant S01. T_{DB} is showing the initial decision boundary after the calibration phase and F_{DB} is showing the change in the decision boundary due to covariate shift adaptation in the online feedback phase. The blue cross ('+' symbols are showing the left MI features and blue circle ('o') symbols are showing the right MI features in the online feedback phase.

current trial and $x_{(i)}$ is the observation in the current trial. By observation we mean here the first principal component of the CSP feature of the current trial. As the EEG features are generally multivariate, it could be misleading to monitor such input processes independently. For example, if the probability of one feature variable to exceed the control limit is 0.0027 then 0.27% of false detection rate is expected. Thus the use of d independent control charts for d independent feature variables can result into highly distorted outcomes. For this reason principal component analysis (PCA) was used to reduce the dimension of the feature vector and a single component was used as the observation $x_{(i)}$ [16]. The CSP feature vector ($Feat_{csp}$ of dimension 1×4) obtained from a particular trial in the online feedback phase is transformed using PCA coefficient matrix $COEFF_{pca}$ (dimension 4×4), calculated from the calibration phase to get the principal components (x_{pcs}).

$$x_{pcs} = COEFF_{pca} \cdot Feat'_{csp} \quad (4)$$

From x_{pcs} , the first principal component is taken as the observation x_i for that trial. Now, the one-step-ahead prediction of $x_{(i)}$ is EWMA $z_{(i-1)}$, from which we can calculate the prediction error as,

$$err_{(i)} = x_{(i)} - z_{(i-1)} \quad (5)$$

Then according to [46] the upper and lower control limits for $x_{(i)}$ can be calculated as,

$$UCL_{(i)} = z_{(i-1)} + L\sigma_{err_{(i-1)}} \quad (6)$$

$$LCL_{(i)} = z_{(i-1)} - L\sigma_{err_{(i-1)}} \quad (7)$$

where, $UCL_{(i)}$ and $LCL_{(i)}$ are the upper and lower control limits respectively for trial i . L is the control limit multiplier. The value of L is chosen to be equal to 2, which is suitable for detecting minor shifts in trial-to-trial transfer [16]. The standard deviation σ_{err} of the one-step ahead error err is

calculated directly using smoothed variance [35] from the following relation,

$$\sigma_{err_{(i)}}^2 = \alpha err_{(i)}^2 + (1 - \alpha)\sigma_{err_{(i-1)}}^2 \quad (8)$$

where, α is the 5% level of significance for the confidence interval of $(1 - \alpha)$.

Finally, $x_{(i)}$ is checked whether it lies within the control limit i.e. $UCL_{(i)} \geq x_{(i)} \geq LCL_{(i)}$. If $x_{(i)}$ falls outside the control limit then only the covariate shift detection(CSD) warning is raised. Once CSD warning is raised, the process goes for the CSD validation in stage-II, to confirm the covariate shift.

The CSD parameters has been generated in the calibration phase, on the basis of which the two stage CSD test detects the trial-to-trial shifts in the online feedback phase. There are mainly four parameters to be obtained after the end of the calibration phase. These are λ , $z_{(0)}$, $\sigma_{err_{(0)}}^2$ and $COEFF_{pca}$. We obtain λ by minimizing the sum of the squared one-step-ahead prediction error, on the data recored during the calibration phase. $z_{(0)}$ is the mean of the observations x in the calibration dataset, $\sigma_{err_{(0)}}^2$ is obtained by dividing the sum of squared one-step-ahead prediction errors by the length of the calibration dataset, and $COEFF_{pca}$ is the PCA coefficient matrix. These four parameters λ , $z_{(0)}$, $\sigma_{err_{(0)}}^2$ and $COEFF_{pca}$ calculated from the calibration phase acts as the initial parameters at the online feedback phase. Later, z and σ_{err}^2 changes trial by trial during the online feedback phase, while λ remains fixed from the calibration phase. L is a parameter in the EEG-CSAC and it is used as the control limit multiplier, which defines the upper and lower limits of the shift-detection boundary. Hence, a small value of L (e.g. $L = 2$) makes the shift-detection test sensitive to minor shifts, which may occur during the trial-to-trial transfer; whereas, a larger value of L (e.g. $L = 3$) is accounted for long-term non-stationaries such as run-to-run or session-to-session [16]. As, in our study the objective is to detect the shift in trial-to-trial transfer, the value of $L = 2$. The same value was chosen

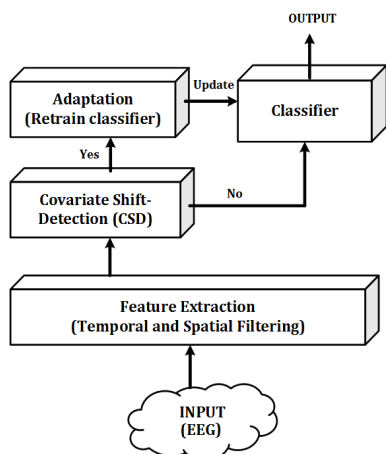


Fig. 4. Interaction between difference modules of the shift detection and classifier adaptation for single trial detection of MI tasks.

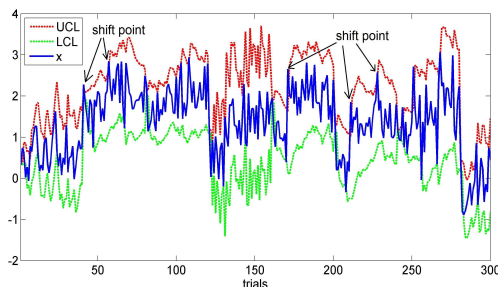


Fig. 5. An example of CSD test is shown from many trials recorded over several participants. Observations (x) from each trial are plotted along with their upper and lower control limits, calculated from the EWMA model. Shift points, detected from the two-stage CSD test are marked with arrows.

experimentally, in our previous study [16], where the same CSD test was applied on offline analysis of BCI competition datasets.

To show the changes in the observation of a particular trial, with and without the shift detection the first principal component of the CSP feature (x_i) has been plotted against the upper (UCL) and lower (LCL) control limit in Fig 5. This figure clearly shows the trials where the x went beyond the control limit for which shift-detection warning has been generated. We picked a chunk of 300 trials over several runs from the recorded datasets to plot the graph in Fig. 5.

b) Covariate Shift Validation (CSV): The stage-II of the two stage CSD test is the CSV and it is executed only if the stage-I (i.e. CSW) raises a shift-detection warning. This stage is introduced to reduce the number of false warnings which leads to unnecessary retraining of the classifier. It relies on the two sets of observations (n_1 and n_2); one which has been generated during training phase (n_1) and another one, which is generated by the CSW instant (n_2). The set n_1 is assumed to be stationary as it is a set of multivariate feature obtained after spatial filtering from the calibration phase and compared with the set n_2 from the current trial at the CSW time point with same number of multivariate features obtained after spatial filtering in online feedback phase. Multivariate Hotelling's T-Squared test [47] is applied to validate the stationarity. The

advantage of using this hypothesis test is that it is a non-parametric test and it can provide a decision whether the two subsequences n_1 and n_2 are stationary with similar means. The Hotelling's T-Square test is based on the equation,

$$HT^2 = (\mu_1 - \mu_2) \left\{ \left(\frac{\Sigma_1}{|n_1|} + \frac{\Sigma_2}{|n_2|} \right) \right\}^{-1} (\mu_1 - \mu_2)' \quad (9)$$

where, Σ_1 and Σ_2 are the covariances and μ_1 and μ_2 are the means of the two subsequences n_1 and n_2 respectively. The lengths of the sub-sequences n_1 and n_2 are denoted as $|n_1|$ and $|n_2|$ respectively. The covariate shift warning is validated only if the p value of the test is less than 0.05 and thus the detection of shift is confirmed.

c) Covariate Shift Adaptation (CSA): Once the CSD is validated, the adaptation phase starts (see Fig. 4). It is assumed that in each trial, the true label is available (as is the case in a rehabilitation application, where the MI instruction is provided with a cue in each trial). The data corresponding to correct labels are appended to the existing training data used for classifier training and the updated data are then used to retrain the classifier. The retrained classifier is then used to classify the upcoming data. On each CSD, the calibration data thus gets updated and a classifier is built and adapted incrementally.

4) Classification and Evaluation Metrics: The performance of the system is measured on the basis of the classification accuracy. The classification accuracy of the SVM pattern classifier f is given in percentage (%). The performance of the CSD test is measured in percentage (%) for the CSW and CSV, which are as given in (10) and (11) respectively.

$$CSW(\%) = \left(\frac{\text{Number of shift detected}}{\text{Total number of trials}} \right) \times 100 \quad (10)$$

$$CSV(\%) = \left(\frac{\text{Number of shift validated}}{\text{Total number of trials}} \right) \times 100 \quad (11)$$

The statistical significance of the results is assessed using the Wilcoxon signed rank test for the pairwise comparison between EEG-NAC and EEG-CSAC at confidence level 0.01.

III. RESULTS

The superiority of the proposed EEG-CSAC method is shown by comparing its decoding accuracy with the conventional EEG-NAC method, both in case of healthy and patient groups. Also the performance of the two-stage CSD algorithm in reducing the false detection by CSV is shown by comparing the percentage of CSW and CSV for each participant. We also investigated the co-relation between CSV and the improvement in accuracy due to EEG-CSAC, to get an idea of how sensitive EEG-CSAC is with respect to the occurrence of the actual covariate-shifts in the streaming data.

The classification accuracies of EEG-NAC and EEG-CSAC for the healthy participant group are shown in Table II and that for patient group are shown in Table III. In case of the EEG-NAC method, the average classification accuracy for the

healthy group was found to be $75.25 \pm 5.46\%$, while for the same group EEG-CSAC method yielded an significantly ($p < 0.01$) increased average accuracy of $81.5 \pm 4.89\%$. In case of the patient group, we obtained an average accuracy of $70.25 \pm 3.43\%$ for EEG-NAC while for the patient group also EEG-CSAC performed significantly ($p < 0.01$) superior with an average accuracy of $75.75 \pm 3.92\%$. The comparison of the classification accuracy distribution for the methods used in the experimental process is shown in Fig. 6 for healthy and patient groups. Tables II & III also show the time-points of feedback trigger in the 5th column with the heading FTTI, i.e. Feedback trigger time instance. The average FTTI for healthy is 6.35 ± 1.06 s and average FTTI of patient is 7.30 ± 0.67 s. A two tailed paired t-test reveals that the healthy group's FTTI is significantly lesser than the patient group's FTTI.

The Kappa values are also calculated apart from the accuracy to highlight the efficiency of the classifiers as sensitivity and specificity measures are implicit in its calculation process and it is also feasible to show the performance for all the participants within a limited space. The comparison of kappa values between the two classifiers also show the significantly (p -value < 0.01) higher performance of EEG-CSAC than EEG-NAC, which further reinforces our claim. The kappa values are shown in Table IV.

TABLE II
CLASSIFICATION ACCURACIES IN HEALTHY GROUP (H)

| Participants | Healthy Group (H) | | | |
|--|-------------------|-----------------|--------------|------|
| | Calibration | Online Feedback | | |
| | 10-CV (%) | EEG-NAC (%) | EEG-CSAC (%) | FTTI |
| S01 | 68.75 | 70.00 | 72.50 | 7 |
| S02 | 75.00 | 85.00 | 87.50 | 4.50 |
| S03 | 87.50 | 80.00 | 82.50 | 7.00 |
| S04 | 82.50 | 75.00 | 80.00 | 8.00 |
| S05 | 87.50 | 77.50 | 80.00 | 6.50 |
| S06 | 87.50 | 80.00 | 87.50 | 6.50 |
| S07 | 75.00 | 75.00 | 82.50 | 6.50 |
| S08 | 67.50 | 70.00 | 82.50 | 5.00 |
| S09 | 87.50 | 67.50 | 85.00 | 5.50 |
| S10 | 66.25 | 72.50 | 75.00 | 7.00 |
| Mean | 78.50 | 75.25 | 81.50 | 6.35 |
| Std | 9.01 | 5.46 | 4.89 | 1.06 |
| p value (between EEG-NAC vs. EEG-CSAC) <0.01 | | | | |

FTTI: Feedback Trigger Time Instant; 10-CV = 10-Fold Cross Validation

Estimation of the information transfer rate (ITR) is also necessary to measure the performance of the system implemented online. Table V shows the ITR for each classifier for all the participants (healthy and patients). The ITR has been calculated in bits/trial according to the formula given in [48].

$$B = \log_2 N + P \log_2 P + (1 - P) \log_2 \frac{1 - P}{N - 1} \quad (12)$$

where, B is the information transfer rate, N = number of classes, P = accuracy (expressed between 0 to 1). Results show that the average increase in the accuracy of 5.88% leads to an average increase in ITR of 9.84%, which is 1.6735 times of the increase in accuracy. This finding is in harmony with

TABLE III
CLASSIFICATION ACCURACIES IN PATIENT GROUP (P)

| Participants | Patient Group (P) | | | |
|--|-------------------|-----------------|--------------|------|
| | Calibration | Online Feedback | | |
| | 10-CV (%) | EEG-NAC (%) | EEG-CSAC (%) | FTTI |
| S01 | 87.50 | 70.00 | 72.50 | 8.00 |
| S02 | 91.25 | 67.50 | 72.50 | 6.50 |
| S03 | 90.00 | 75.00 | 82.50 | 7.50 |
| S04 | 77.50 | 65.00 | 72.50 | 7.50 |
| S05 | 91.25 | 75.00 | 77.50 | 6.00 |
| S06 | 91.25 | 67.50 | 72.50 | 7.00 |
| S07 | 68.75 | 67.50 | 75.00 | 8.00 |
| S08 | 78.75 | 72.50 | 75.00 | 7.50 |
| S09 | 53.75 | 72.50 | 82.50 | 8.00 |
| S10 | 66.25 | 70.00 | 75.00 | 7.00 |
| Mean | 79.63 | 70.25 | 75.75 | 7.30 |
| Std | 13.11 | 3.43 | 3.92 | 0.67 |
| p value (between EEG-NAC vs. EEG-CSAC) <0.01 | | | | |

FTTI: Feedback Trigger Time Instant; 10-CV = 10-Fold Cross Validation

TABLE IV
KAPPA VALUES IN HEALTHY (H) AND PATIENT (P) GROUPS

| Participants | Healthy Group (H) | | Patient Group (H) | |
|--------------|-------------------|----------|-------------------|----------|
| | EEG-NAC | EEG-CSAC | EEG-NAC | EEG-CSAC |
| S01 | 0.40 | 0.45 | 0.40 | 0.45 |
| S02 | 0.70 | 0.75 | 0.35 | 0.45 |
| S03 | 0.60 | 0.65 | 0.50 | 0.65 |
| S04 | 0.50 | 0.60 | 0.30 | 0.45 |
| S05 | 0.55 | 0.60 | 0.50 | 0.55 |
| S06 | 0.60 | 0.75 | 0.35 | 0.45 |
| S07 | 0.50 | 0.65 | 0.35 | 0.50 |
| S08 | 0.40 | 0.65 | 0.45 | 0.50 |
| S09 | 0.35 | 0.70 | 0.45 | 0.65 |
| S10 | 0.45 | 0.50 | 0.40 | 0.50 |
| Mean | 0.51 | 0.63 | 0.41 | 0.52 |
| Std | 0.10 | 0.09 | 0.06 | 0.07 |

the argument provided in [48], that a slight improvement in accuracy can influence the information transfer rate to a great extent.

The choices of the smoothing constant λ for the CSD tests are given in Table VI (2nd column) & Table VII (2nd column) for healthy and patient groups respectively. The results of CSW & CSV are shown in the 3rd and 4th columns of the Table VI & Table VII, respectively for healthy and patient groups. The average rate of CSW in healthy group was found as $15.75 \pm 5.65\%$, while in the patient group it was $16.75 \pm 2.89\%$. However, after the CSV at stage II, the rate of CSD reduced significantly ($p < 0.01$), as the average CSV rates for healthy group and patient group were 9.25 ± 3.54 and 9 ± 2.10 respectively. We also investigated the correlation between the variation of accuracy difference between EEG-CSAC and EEG-NAC and the variation in CSV rates, which reveals that there is a positive correlation ($r = 0.853$, $p < 0.01$) between these two quantities, as seen in Fig. 7. The CSV rate and accuracy difference between EEG-NAC and EEG-CSAC are shown in Table VIII for all participants across the two participant groups.

TABLE V
THE ITRS FOR TWO DIFFERENT CLASSIFIERS ACROSS ALL THE PARTICIPANTS

| Group | Participants | ITR(bits/trial) | | |
|----------|--------------|-----------------|----------|------------|
| | | EEG-NAC | EEG-CSAC | Difference |
| Healthy | S01 | 0.1187 | 0.1515 | 0.0327 |
| | S02 | 0.3902 | 0.4564 | 0.0663 |
| | S03 | 0.2781 | 0.3310 | 0.0529 |
| | S04 | 0.1887 | 0.2781 | 0.0894 |
| | S05 | 0.2308 | 0.2781 | 0.0473 |
| | S06 | 0.2781 | 0.4564 | 0.1784 |
| | S07 | 0.1887 | 0.3310 | 0.1423 |
| | S08 | 0.1187 | 0.3310 | 0.2123 |
| | S09 | 0.0903 | 0.3902 | 0.2999 |
| | S10 | 0.1515 | 0.1887 | 0.0373 |
| Patients | S01 | 0.1187 | 0.1515 | 0.0327 |
| | S02 | 0.0903 | 0.1515 | 0.0612 |
| | S03 | 0.1887 | 0.3310 | 0.1423 |
| | S04 | 0.0659 | 0.1515 | 0.0855 |
| | S05 | 0.1887 | 0.2308 | 0.0421 |
| | S06 | 0.0903 | 0.1515 | 0.0612 |
| | S07 | 0.0903 | 0.1887 | 0.0985 |
| | S08 | 0.1515 | 0.1887 | 0.0373 |
| | S9 | 0.1515 | 0.3310 | 0.1795 |
| | S10 | 0.1187 | 0.1887 | 0.0700 |
| | Mean | 0.1644 | 0.2629 | 0.0984 |

TABLE VI
 λ VALUES AND CSD TEST METRICS IN HEALTHY (H) GROUP

| Participants | Healthy Group | | |
|--|------------------|------------|------------|
| | lambda λ | CSW in (%) | CSV in (%) |
| S01 | 0.10 | 10.00 | 7.50 |
| S02 | 0.80 | 7.50 | 5.00 |
| S03 | 0.20 | 10.00 | 7.50 |
| S04 | 0.10 | 20.00 | 7.50 |
| S05 | 0.10 | 12.50 | 7.50 |
| S06 | 0.10 | 20.00 | 12.50 |
| S07 | 0.70 | 15.00 | 12.50 |
| S08 | 0.30 | 17.50 | 12.50 |
| S09 | 0.90 | 25.00 | 15.00 |
| S10 | 0.20 | 20.00 | 5.00 |
| Mean | 0.35 | 15.75 | 9.25 |
| Std | 0.32 | 5.65 | 3.54 |
| p-value (CSW vs. CSV) < 0.01 | | | |

IV. DISCUSSION

The results produced by the experiments prove two major claims made in the paper. The first is that EEG-CSAC based online adaptation leads to superior performance of the BCI system in terms of classification accuracy ($p < 0.01$), as compared to the conventional EEG-NAC method. The fact that it occurred both in the case of healthy as well as patient groups, establishes the robustness of the method. The second is that the two-stage covariate shift detection test significantly ($p < 0.01$) reduced the number of re-training of the classifier in a single run of the online BCI. As each time a valid shift is detected, the classifier needs to be re-trained; the CSV values in Table VI & Table VII show the requirement of classifier re-training for each participant. Similarly, CSW values in Table VI & Table VII show the re-training requirement of the classifier without using the second stage of the two-stage CSD

TABLE VII
 λ VALUES AND CSD TEST METRICS IN PATIENT (P) GROUP

| Participants | Patient Group | | |
|--|------------------|------------|------------|
| | lambda λ | CSW in (%) | CSV in (%) |
| S01 | 0.1 | 20.00 | 7.50 |
| S02 | 0.3 | 15.00 | 7.50 |
| S03 | 0.2 | 15.00 | 10.00 |
| S04 | 1.0 | 20.00 | 12.50 |
| S05 | 0.7 | 12.50 | 7.50 |
| S06 | 0.1 | 12.50 | 7.50 |
| S07 | 0.1 | 17.50 | 12.50 |
| S08 | 0.3 | 17.50 | 7.50 |
| S09 | 0.2 | 17.50 | 100 |
| S10 | 0.2 | 20.00 | 7.50 |
| Mean | 0.32 | 16.75 | 9.00 |
| Std | 0.2974 | 2.89 | 2.1 |
| p-value (CSW vs. CSV) < 0.01 | | | |

TABLE VIII
RELATION BETWEEN EEG-NAC TO EEG-CSAC ACCURACY IMPROVEMENT AND CSV FOR HEALTHY (H) AND PATIENTS (P) GROUPS

| Group | Subject | CSW in (%) | EEG-NAC to EEG-CSAC change(%) |
|----------|---------|------------|-------------------------------|
| Healthy | S01 | 7.50 | 2.50 |
| | S02 | 5.00 | 2.50 |
| | S03 | 7.50 | 2.50 |
| | S04 | 7.50 | 5.00 |
| | S05 | 7.50 | 2.50 |
| | S06 | 12.50 | 7.50 |
| | S07 | 12.50 | 7.50 |
| | S08 | 12.50 | 12.50 |
| | S09 | 15.00 | 17.50 |
| | S10 | 5.00 | 2.50 |
| Patients | S01 | 7.5 | 2.50 |
| | S02 | 7.50 | 5.00 |
| | S03 | 10.00 | 7.50 |
| | S04 | 12.50 | 7.50 |
| | S05 | 7.50 | 2.50 |
| | S06 | 7.50 | 5.00 |
| | S07 | 12.50 | 7.50 |
| | S08 | 7.50 | 2.50 |
| | S9 | 10.00 | 10.00 |
| | S10 | 7.50 | 5.00 |

test. It's worth mentioning that the comparison between CSW and CSV values reveal that the introduction of the second stage significantly reduced the need for classifier re-training. This two-stage CSD test serves two important purposes; 1) it reduces the delay in system by avoiding unnecessary retraining and 2) it minimizes the risk for inappropriate adaptation of the classifier during the online feedback phase, which is one of the major concerns of adaptive BCI technique[13]. The difference between healthy and patient groups in terms of FTTI suggests that healthy participants' MI-activation, related to cue presentation, was quicker than the patients'. This is also expected, as in patients brain lesions may disturb the brain networks responsible for the MI. Additionally, it may be possible that the patients tend to get more fatigued than the healthy participants during the experiments which may lead to such delayed response. Moreover, we investigated how susceptible is the performance of the newly proposed EEG-

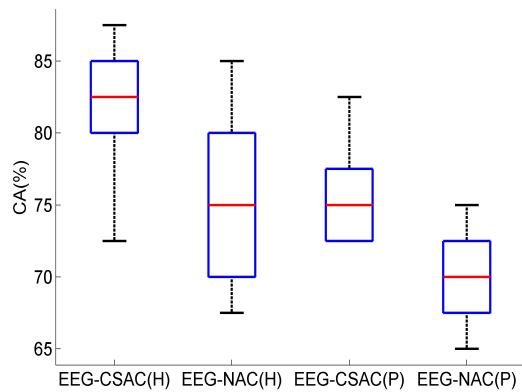


Fig. 6. Comparison of classifier performance in Healthy(EEG-CSAC(H) and EEG-NAC(H)) and Patient(EEG-CSAC(P) and EEG-NAC(P)) groups

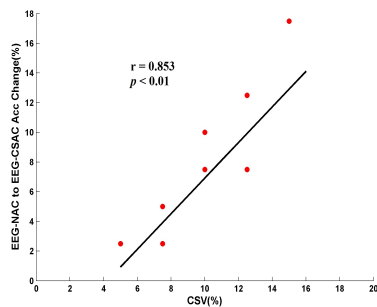


Fig. 7. Correlation between EEG-NAC to EEG-CSAC accuracy improvement and CSV. Red dots indicating the data for each participant and the black line drawn is the linear-least-square estimate of the data distribution.

CSAC method to the detection of covariate shifts. To this end we have computed the correlation between the number of covariate shifts that occurred in a particular run of the online BCI, and the improvement in accuracy due to classifier adaptation, which showed a significantly high correlation ($r = 0.853$, $p < 0.01$). This establishes the fact that the covariate shifts were correctly estimated and the classifiers were appropriately updated leading to the improvements in the accuracy and thus the covariate shift adaptation was in general meaningful and robust.

The CSD-based adaptive online BCI system, proposed here requires a total of 16 min of calibration time which is comparable to the other adaptive BCIs found in literature [49]. Mutual learning is also promoted in the current implementation of adaptive BCI system by introducing visual as well as proprioceptive neurofeedback [9]. The visual feedback is anthropomorphic and plays a key role in neurorehabilitation as it is related to the activation of action-observation networks [50]. The motor imagery activated proprioceptive feedback (by moving the patient’s paretic fingers with the help of the hand-exoskeleton), also engages the neurons in the neighboring areas of the lesion, through intact afferent pathways [51]. Thus simultaneous application of both of these modes of giving neurofeedback is very important for stroke patients in recovering lost motor skills. The computation cost associated with the two-stage CSD test and classifier adaptation

is in milliseconds, using a standard mobile workstations and a MATLAB/Simulink platform, therefore it can be easily extended for generating continuous feedback, (although in the current study it is one time in a trial). The fact that the EEG-CSAC based online BCI enabled all the healthy and stroke participants to trigger the hand-exoskeleton by their motor imagery task with satisfactory levels of accuracy, which are superior ($p < 0.01$) to that obtained with EEG-NAC, clearly demonstrates the effectiveness of the technique in adapting to the non-stationarity of the brain-waves and providing neurofeedback with enhanced accuracy. Here the non-stationarity includes changes from calibration to online feedback generation stage as well as inter-trial changes within a single run of the online BCI. Several studies have tried to improve the power of CSP-based BCIs by introducing KL divergence based loss functions to minimize within class mismatching [26] or optimizing CSP algorithm [20]. Time series prediction and adaptive auto-regression based feature extraction were also investigated to minimise the adverse effect of non-stationarity in BCI [52]. While these studies focus in finding features that are invariant to non-stationary effects; our attempt is to take conventional feature extraction methods and try to update the classifier with the occurrence of covariate shifts. The advantage is that our method is independent of what feature extraction technique is used. Similar approaches are already popular to make adaptive BCI systems [29], [17], [32], [22], [18]. Although our approach have some resemblance to a recent off-line study where EWMA based adaptive processing is used before stack regularized LDA based classification [53], the two-stage CSD test and classifier updating strategy are novel in the current work. Also here it is implemented in online BCI and its feasibility is tested on stroke patients. However, Alonso et al. validated their algorithm on multiclass decoding, whereas our current work is implemented on binary classification [53]. Hence, there is further scope for extending it to multiclass decoding. Indeed both of the methods dealt with the temporal variability considering different time segments, but unlike Alonso et al. the subject specific frequency variability is not considered in the current work, rather the frequency bands [8 – 12] Hz and [16 – 24] Hz are kept fixed for all the participants. The main reason was to keep the method simple and to focus on the validity of the CSD-based adaptation in online BCI. A direct comparison of classification accuracies with other adaptive BCI systems is not possible as it is difficult to produce exact experimental conditions for each one of them. Therefore we took a state-of-the-art conventional CSP-based non-adaptive classification method, EEG-NAC for comparing the performance of the current EEG-CSAC algorithm.

In online studies the scope of pre-processing is generally limited as it increases the time complexity of the system and reduces the speed of response. Therefore the classification accuracy sometimes gets heavily affected due to contamination of artifacts and external noises. It can be seen in the Tables II-III, that the classification accuracy dropped below 70% for a few participants in EEG-NAC. The CSP-based spatial filtering technique was used here as it improves the signal to noise ratio in the data and increases inter-class feature separability. Although PCA-based dimensionality reduction may have neg-

ative effects on the EEG data quality as it lumps the variance, but Xiao and Ding 2013 [54] used PCA-based spectral features in successfully decoding individual finger movements from EEG. The CSD-based adaptation approach proposed here is supervised in nature as we implemented synchronous online BCI, where the label of a particular trial is known before hand and we assumed full compliance with cues. As this assumption may be questionable, partially supervised adaptation using a well-known technique of Error-Potentials can be explored in conjunction with CSD for better performance [22].

Future work may include extending the proposed EEG-CSAC based adaptive online BCI for continuous control with increased information transfer rate to generate smoother feedback. Also the current scope of synchronous BCI may be extended to asynchronous cases for more practical use in activities of daily living using assistive technologies.

V. CONCLUSION

The paper implements an online BCI system with a two-stage CSD test based classifier adaptation. The online BCI system, capable of generating MI triggered visual and hand exoskeleton based neurofeedback, was tested for its practical feasibility and effectiveness on both healthy individuals and stroke patients. In comparison to the conventional CSP-based non-adaptive method, EEG-CSAC performed significantly better in terms of classification accuracy. The classification accuracy improvements strongly correlated with the number of validated CSD occurrences, further proving the consistency of EEG-CSAC algorithm. The two-stage CSD test comprising of EWMA test and Hotellings T-square statistical test was demonstrated to be effective in reducing the false detection rate and thereby preventing unnecessary adaptation of the classifier. Overall, the EEG-CSAC has been proven to be a practical and significantly superior method for designing adaptive BCI based hand-exoskeleton integrated neurorehabilitation therapies for stroke patients.

ACKNOWLEDGMENT

This work is supported by Department of Science and Technology (DST), India and UK India Education and Research Initiative (UKIERI) Thematic Partnership project "A BCI operated hand exoskeleton based neurorehabilitation system" (UKIERI-DST-20130354). We also thank Regency Hospital, Kanpur, India to enable the experiments on stroke patients.

REFERENCES

- [1] J. J. Vidal, "Toward Direct Brain-Computer Communication," *Annu. Rev. Biophys.*, vol. 2, no. 1, pp. 157–180, Jun. 1973.
- [2] G. Dornhege, *Toward brain-computer interfacing*. MIT press, 2007.
- [3] N. Birbaumer, A. Kübler, N. Ghanayim, T. Hinterberger, J. Perelmouter, J. Kaiser, I. Iversen, B. Kotchoubey, N. Neumann, and H. Flor, "The thought translation device (TTD) for completely paralyzed patients," *IEEE Trans. Neural Syst. Rehabil. Eng.*, vol. 8, no. 2, pp. 190–193, 2000.
- [4] G. Prasad, P. Herman, D. Coyle, S. McDonough, and J. Crosbie, "Applying a brain-computer interface to support motor imagery practice in people with stroke for upper limb recovery: a feasibility study," *J. Neuroeng. Rehabil.*, vol. 7, no. 1, p. 60, 2010.
- [5] V. Crocher, A. Sahbani, J. Robertson, A. Roby-Brami, and G. Morel, "Constraining upper limb synergies of hemiparetic patients using a robotic exoskeleton in the perspective of neuro-rehabilitation," *IEEE Trans. Neural Syst. Rehabil. Eng.*, vol. 20, no. 3, pp. 247–257, 2012.
- [6] M. A. Dimyan and L. G. Cohen, "Neuroplasticity in the context of motor rehabilitation after stroke," *Nature reviews. Neurology*, vol. 7, no. 2, pp. 76–85, 2011.
- [7] H. Cecotti, "Spelling with non-invasive Brain-Computer Interfaces—current and future trends," *Journal of physiology, Paris*, vol. 105, no. 1–3, pp. 106–14, 2011.
- [8] J. Ueda, D. Ming, V. Krishnamoorthy, M. Shinohara, and T. Ogasawara, "Individual muscle control using an exoskeleton robot for muscle function testing," *IEEE Transactions on Neural Systems and Rehabilitation Engineering*, vol. 18, no. 4, pp. 339–350, 2010.
- [9] A. Ramos-Murguialday, M. Schürholz, V. Caggiano, M. Wildgruber, A. Caria, E. M. Hammer, S. Halder, and N. Birbaumer, "Proprioceptive Feedback and Brain Computer Interface (BCI) Based Neuroprostheses," *PLoS ONE*, vol. 7, no. 10, 2012.
- [10] A. Chowdhury, H. Raza, A. Dutta, S. S. Nishad, A. Saxena, and G. Prasad, "A Study on Cortico-muscular Coupling in Finger Motions for Exoskeleton Assisted Neuro-Rehabilitation," in *Proc. 37th Annual International Conference of the IEEE Engineering in Medicine and Biology Society (EMBC), 2015*, 2015, pp. 4610–4614.
- [11] A. Chowdhury, H. Raza, A. Dutta, and G. Prasad, "Eeg-emg based hybrid brain computer interface for triggering hand exoskeleton for neuro-rehabilitation," in *Proc. of the Advances in Robotics*, Jun. 2017, pp. 45:1–45:6.
- [12] J. Zhao, W. Li, X. Mao, H. Hu, L. Niu, and G. Chen, "Behavior-based ssvp hierarchical architecture for telepresence control of humanoid robot to achieve full-body movement," *IEEE Transactions on Cognitive and Developmental Systems*, vol. 9, no. 2, pp. 197–209, Jun. 2017.
- [13] J. R. Wolpaw, N. Birbaumer, D. J. McFarland, G. Pfurtscheller, and T. M. Vaughan, "Brain-Computer Interfaces for Communication and Control," *Clinical Neurophysiology : Official Journal of the International Federation of Clinical Neurophysiology*, vol. 113, no. 6, pp. 767–91, Jun. 2002.
- [14] Y. Jiang, N. T. Hau, and W. Y. Chung, "Semi-asynchronous bci using wearable two-channel eeg," *IEEE Transactions on Cognitive and Developmental Systems*, vol. PP, no. 99, pp. 1–1, 2017.
- [15] D. Rathee, H. Raza, G. Prasad, and H. Cecotti, "Current source density estimation enhances the performance of motor-imagery-related brain-computer interface," *IEEE Trans. on Neural Syst. and Rehab. Eng.*, vol. 25, no. 12, pp. 2461–2471, Dec. 2017.
- [16] H. Raza, H. Cecotti, Y. Li, and G. Prasad, "Adaptive learning with covariate shift-detection for motor imagery-based braincomputer interface," *Soft Computing*, vol. 20, no. 8, pp. 3085–3096, Aug. 2016.
- [17] P. Shenoy, M. Krauledat, B. Blankertz, R. P. N. Rao, and K.-R. Müller, "Towards adaptive classification for BCI," *J. Neural Eng.*, vol. 3, no. 1, pp. R13–R23, Mar. 2006.
- [18] Y. Li, H. Kambara, Y. Koike, and M. Sugiyama, "Application of covariate shift adaptation techniques in brain-computer interfaces," *IEEE Transactions on Biomedical Engineering*, vol. 57, no. 6, pp. 1318–1324, Jun. 2010.
- [19] B. Blankertz, G. Dornhege, M. Krauledat, K. R. Müller, and G. Curio, "The non-invasive Berlin Brain-Computer Interface: Fast acquisition of effective performance in untrained subjects," *NeuroImage*, vol. 37, no. 2, pp. 539–550, 2007.
- [20] B. Blankertz, R. Tomioka, S. Lemm, M. Kawanabe, and K. R. Müller, "Optimizing spatial filters for robust EEG single-trial analysis," *IEEE Signal Processing Magazine*, vol. 25, no. 1, pp. 41–56, 2008.
- [21] P. Y. Zhou and K. C. C. Chan, "Fuzzy feature extraction for multi-channel eeg classification," *IEEE Transactions on Cognitive and Developmental Systems*, vol. PP, no. 99, pp. 1–1, 2016.
- [22] A. Butfield, P. W. Ferrez, and J. D. R. Millán, "Towards a robust BCI: Error potentials and online learning," *IEEE Trans. Neural Syst. Rehabil. Eng.*, vol. 14, no. 2, pp. 164–168, Jun. 2006.
- [23] C. Vidaurre, A. Schlögl, R. Cabeza, R. Scherer, and G. Pfurtscheller, "Study of on-line adaptive discriminant analysis for EEG-based brain computer interfaces," *IEEE Trans. on Biomed. Eng.*, vol. 54, no. 3, pp. 550–556, 2007.
- [24] X. Liao, D. Yao, and C. Li, "Transductive SVM for reducing the training effort in BCI," *Journal of neural engineering*, vol. 4, no. 3, pp. 246–54, Sep. 2007.
- [25] H. Raza, H. Cecotti, Y. Li, and G. Prasad, "Learning with Covariate Shift-Detection and Adaptation in Non-Stationary Environments : Application to Brain-Computer Interface," in *Proc. 2015 International Joint Conference on Neural Networks (IJCNN)*, 2015, pp. 1–8.

- [26] M. Arvaneh, C. Guan, K. K. Ang, and C. Quek, "Optimizing spatial filters by minimizing within-class dissimilarities in electroencephalogram-based brain-computer interface," *IEEE Trans. Neural Netw. Learn. Syst.*, vol. 24, no. 4, pp. 610–619, 2013.
- [27] P. A. Herman, G. Prasad, and T. M. McGinnity, "Designing an interval type-2 fuzzy logic system for handling uncertainty effects in brain-computer interface classification of motor imagery induced eeg patterns," *IEEE Trans. on Fuzzy Syst.*, vol. 25, no. 1, pp. 29–42, Feb. 2017.
- [28] H. Raza, H. Cecotti, and G. Prasad, "Optimising Frequency Band Selection with Forward-Addition and Backward-Elimination Algorithms in EEG-based Brain-Computer Interfaces," in *Proc. 2015 International Joint Conference on Neural Networks (IJCNN)*, 2015, pp. 1–7.
- [29] A. Satti, C. Guan, D. Coyle, and G. Prasad, "A covariate shift minimization method to alleviate non-stationarity effects for an adaptive brain-computer interface," in *Proc. International Conference on Pattern Recognition*, Aug. 2010, pp. 105–108.
- [30] H. Raza, G. Prasad, Y. Li, and H. Cecotti, "Covariate shift-adaptation using a transductive learning model for handling non-stationarity in EEG based brain-computer interfaces," in *Proc. 2014 IEEE International Conference on Bioinformatics and Biomedicine (BIBM)*, Nov. 2014, pp. 230–236.
- [31] G. Ditzler, M. Roveri, C. Alippi, and R. Polikar, "Learning in Nonstationary Environments : a Survey," *IEEE Comput. Intell. Mag.*, vol. 10, no. 4, pp. 12–25, 2015.
- [32] C. Vidaurre, A. Schlögl, R. Cabeza, R. Scherer, and G. Pfurtscheller, "A fully on-line adaptive BCI," *IEEE Trans. on Biomed. Eng.*, vol. 53, no. 6, pp. 1214–1219, 2006.
- [33] S. Sun, C. Zhang, and D. Zhang, "An experimental evaluation of ensemble methods for EEG signal classification," *Pattern Recognit. Lett.*, vol. 28, no. 15, pp. 2157–2163, 2007.
- [34] S. R. Liyanage, C. Guan, H. Zhang, K. K. Ang, J. Xu, and T. H. Lee, "Dynamically weighted ensemble classification for non-stationary EEG processing," *Journal of neural engineering*, vol. 10, no. 3, p. 036007, Apr. 2013.
- [35] H. Raza, G. Prasad, and Y. Li, "EWMA model based shift-detection methods for detecting covariate shifts in non-stationary environments," *Pattern Recognition*, vol. 48, no. 3, pp. 659–669, Aug. 2015.
- [36] —, "EWMA based two-stage dataset shift-detection in non-stationary environments," in *Proc. IFIP Advances in Information and Communication Technology*, Oct. 2013, pp. 625–635.
- [37] F. Quandt, C. Reichert, H. Hinrichs, H. J. Heinze, R. T. Knight, and J. W. Rieger, "Single trial discrimination of individual finger movements on one hand: A combined MEG and EEG study," *NeuroImage*, vol. 59, no. 4, pp. 3316–3324, 2012.
- [38] J. Höhne, E. Holz, P. Staiger-Sälzer, K. R. Müller, A. Kübler, and M. Tangermann, "Motor imagery for severely motor-impaired patients: Evidence for brain-computer interfacing as superior control solution," *PLoS ONE*, vol. 9, no. 8, 2014.
- [39] Y. K. Meena, A. Chowdhury, H. Cecotti, S. S. Nishad, A. Dutta, and G. Prasad, "EMOHEX : An Eye Tracker based Mobility and Hand Exoskeleton Device for Assisting Disabled People," in *Proc. 2016 IEEE International Conference on Systems, Man, and Cybernetics (SMC)*, 2016, pp. 2122–2127.
- [40] R. Beisteiner, C. Windischberger, R. Lanzenberger, V. Edward, R. Cunningham, M. Erdler, A. Gartus, B. Streibl, E. Moser, and L. Deecke, "Finger somatotopy in human motor cortex," *NeuroImage*, vol. 13, no. 6 Pt 1, pp. 1016–26, 2001.
- [41] T. Ball, A. Schreiber, B. Feige, M. Wagner, C. H. Lücking, and R. Kristeva-Feige, "The role of higher-order motor areas in voluntary movement as revealed by high-resolution EEG and fMRI," *NeuroImage*, vol. 10, no. 6, pp. 682–94, 1999.
- [42] H. M. Hodkinson, "Evaluation of a mental test score for assessment of mental impairment in the elderly," *Age & Ageing*, vol. 1, no. 4, pp. 233–238, 1972.
- [43] G. Pfurtscheller and F. H. Lopes Da Silva, "Event-related EEG/MEG synchronization and desynchronization: Basic principles," *Clinical Neurophysiology*, vol. 110, no. 11, pp. 1842–1857, 1999.
- [44] H. Ramoser, J. Müller-Gerking, and G. Pfurtscheller, "Optimal spatial filtering of single trial EEG during imagined hand movement," *IEEE Transactions on Rehabilitation Engineering*, vol. 8, no. 4, pp. 441–446, Dec. 2000.
- [45] H. Raza, G. Prasad, and Y. Li, "Dataset shift detection in non-stationary environments using EWMA charts," in *Proc. 2013 IEEE International Conference on Systems, Man, and Cybernetics (SMC)*, 2013, pp. 3151–3156.
- [46] D. Montgomery and C. Mastrangelo, "Some Statistical Process Control Methods for Autocorrelated Data," *Journal of Quality Technology*, vol. 23, no. 3, pp. 179–204, 1991.
- [47] H. Hotelling, "Multivariate Quality Control-Illustrated by the Air Testing of Sample Bombsights," in *Techniques of Statistical Analysis*. New York: McGraw-Hill, 1947, ch. II, pp. 111–184.
- [48] B. Obermaier, C. Neuper, C. Guger, and G. Pfurtscheller, "Information transfer rate in a five-classes brain-computer interface," *IEEE Trans. on Neural Syst. and Rehab. Eng.*, vol. 9, no. 3, pp. 283–288, Sept 2001.
- [49] K. K. Ang, C. Guan, C. Wang, K. S. Phua, A. Hock, G. Tan, and Z. Y. Chin, "Calibrating EEG-based motor imagery brain-computer interface from passive movement," in *Proc. 2011 Annual International Conference of the IEEE in Engineering in Medicine and Biology Society, EMBC*, 2011, pp. 4199–4202.
- [50] S. T. Foldes, D. J. Weber, and J. L. Collinger, "MEG-based neurofeedback for hand rehabilitation," *J. Neuroeng. Rehabil.*, vol. 12, no. 1, p. 85, 2015.
- [51] T. Pistohl, D. Joshi, G. Ganesh, A. Jackson, and K. Nazarpour, "Artificial Proprioceptive Feedback for Myoelectric Control," *IEEE Trans. Neural Syst. Rehabil. Eng.*, vol. 23, no. 3, pp. 498–507, 2014.
- [52] D. Coyle, G. Prasad, and T. M. McGinnity, "A time-series prediction approach for feature extraction in a brain-computer interface," *IEEE Trans. Neural Syst. Rehabil. Eng.*, vol. 13, no. 4, pp. 461–467, 2005.
- [53] L. F. Nicolas-alonso, S. Member, R. Corrales, S. Member, J. Gomez-pilar, D. Álvarez, R. Hornero, and S. Member, "Adaptive Stacked Generalization for Multiclass Motor Imagery-Based Brain Computer Interfaces," *IEEE Trans. Neural Syst. Rehabil. Eng.*, vol. 23, no. 4, pp. 702–712, 2015.
- [54] R. Xiao and L. Ding, "Evaluation of EEG features in decoding individual finger movements from one hand," *Comput. Math. Methods Med.*, vol. 2013, Apr. 2013.